Received 21 September 2023, accepted 17 October 2023, date of publication 23 October 2023, date of current version 1 November 2023.

Digital Object Identifier 10.1109/ACCESS.2023.3326442

RESEARCH ARTICLE

Practical Fixed-Time Adaptive NN Fault-Tolerant Control for Underactuated AUVs With Input Quantization and Unknown Dead Zone

HUARAN YAN[1], YINGJIE XIAO[1], AND HONGGANG ZHANG[2]
[1]Merchant Marine College, Shanghai Maritime University, Shanghai 201306, China
[2]Maritime College, Zhejiang Ocean University, Zhoushan, Zhejiang 316022, China

Corresponding author: Huaran Yan (huaranyan202202@163.com)

This work was supported in part by the National Natural Science Foundation of China under Grant 52071201.

ABSTRACT In this article, a practical fixed-time adaptive neural network (NN) trajectory tracking control scheme for underactuated autonomous underwater vehicles (AUVs) subject to uncertain dynamics, unknown time-varying disturbances, an unknown dead zone, actuator faults and input quantization is developed for the first time. Here, a hysteresis quantizer is introduced to decrease the oscillation in the signal quantization process. Then, the radial basis function NN is employed to compensate the uncertainty term in the AUVs trajectory tracking control system. By incorporating the bounded estimate, smoothing functions and parameter adaptive technique, the problem of unknown dead zone, actuator fault and input quantization are addressed. The restrictive conditions of boundedness for the disturbance-like item in conventional sector bounded quantizer is resolved. Subsequently, a practical fixed-time adaptive NN trajectory tracking control law is designed does not require any parameter information of the quantizer under the backstepping design framework. The theoretical analysis further confirms that all signals in the AUV trajectory tracking closed-loop control system remain bounded, and the developed control scheme is shown to be effective through simulation results.

INDEX TERMS Underactuated AUVs, fault-tolerant control, quantized control, fixed-time control, unknown dead zone.

I. INTRODUCTION

In recent decades, there has been remarkable progress in the exploitation of marine resources. Among various research areas, the trajectory tracking control of autonomous underwater vehicles (AUVs) has gained much attention from scholars. This trajectory tracking control has played a valuable role in critical offshore operations such as ocean exploration, marine transportation, and ocean surveying [1], [2], [3]. However, AUVs face inherent challenges in dealing with uncertain dynamics and encountering unknown time-varying disturbances caused by the vast ocean environment. It is important to emphasize that the exact model parameters of AUVs cannot be directly used for the design of control laws.

To cope with these challenges, various effective approaches have been proposed to ensure the stability and enhance the robustness of trajectory tracking control systems. Different types of disturbance observers have been constructed to compensate for uncertainties, including external environmental disturbances and uncertainties in model parameters [4], [5], [6]. These observers have played a key role in estimating and counteracting the effects of these uncertainties. Furthermore, a parametric adaptive approach has been developed within the backstepping framework to mitigate the uncertain model parameters and unknown environmental disturbances [7], [8], [9]. The focus of this approach is to weaken the effects of these uncertainties. With the aid of intelligent algorithms such as adaptive neural networks (NN) control [10], [11], composite adaptive NN [12] and fuzzy logic systems (FLS) [13], [14], the unknown

The associate editor coordinating the review of this manuscript and approving it for publication was Jinquan Xu.

dynamics or disturbances of the system can be addressed, thus improving the control performance.

In practice, the majority of AUVs are underactuated, which clearly indicates that the number of actuators of an AUV is less than the number of its degrees of freedom (DOF). Up to now, the underactuated AUVs tracking control problem has attracted significant attention. Several effective control schemes have been proposed in the existing literature to deal with this problem, including additional control methods [15], [16], output redefinition control methods [17], line of sight (LOS) methods [18], [19], etc.

It is valuable to indicate that the above literature mainly aims to ensure that the tracking error is uniformly bounded, i.e., the tracking error cannot converge to a finite time. Various finite-time (FT) control schemes have been proposed in [20], [21], and [22]. However, the settling time function in the FT control scheme relies on the initial conditions of the system. Recently, a number of fixed-time control schemes [23], [24] have been devised in which the settling time is independent of the initial conditions of the system. In [23], an NDO-based fixed-time sliding control scheme was designed for formation control of underactuated AUVs. A fixed-time trajectory tracking law with prescribed performance for underactuated AUVs suffering from unknown disturbances and uncertain dynamic was proposed in [24]. A distributed adaptive fixed-time platoon control problem for third-order fully heterogeneous nonlinear vehicles was investigated in [25].

From a practical point of view, AUVs may suffer from corrosion and wear of the actuator due to prolonged underwater operation, and these may lead to the actuator failure with insufficient torque to threaten navigational safety. To deal with the actuator fault problem, fault-tolerant control has gained tremendous attention from the academic community. Loss of effectiveness (LOE) [26] and bias faults [27] are the main concerns for the problem of fault-tolerant tracking control for AUVs. The fault-tolerant tracking control problem for AUVs subject to actuator faults and time-varying ocean disturbances was solved in [26]. In [27], a model-parameter-free control scheme was developed for AUVs with actuator faults and external disturbances. A distributed fault-tolerant control scheme was proposed in [28] to address the effects of actuator failures and various uncertainties on the system performance, while avoiding the over-parameterization problem in adaptive control methods.

The dead zone of an actuator also indicates the insensitive zone of the actuator. It is a finite interval in which a change in input does not cause any perceptible change in the actuator. Typically, dead zone is caused by friction between components within the instrument and the actuation accuracy of the components. The unknown dead zone is one of the most classic non-smooth actuator nonlinearities and is typically found in various practical systems [29], [30], [31], [32]. It is vital to overcome the effects of dead zones due to which their existence can damage the control performance of the engineering system [29]. To solve the attitude tracking control of helicopter in the presence of unknown dead zones, a state feedback control law was developed by [30]. For a nonlinear system with dead zone, an adaptive finite-time trajectory tracking control law was constructed by [31]. To cope with the influence of dead zone for robotic manipulators, an adaptive NN control law was proposed in [32].

As known as a typical networked system, the transfer of information between components takes place over a communication channel. For the information to be transmitted in the channel, it has to be quantization and encoded first. Quantization is a technique that transforms a continuous signal into a segmented constant signal according to a specific transformation algorithm, and the quantization problem studied in this paper focuses on the quantization of the control inputs signal in the system (information transmitted between the controller and actuator), i.e., input quantization. The quantization of the input signal is a problem which makes it more difficult to achieve stability than a system without quantization [33], [34], [35], [36]. Quantizer is always needed in the process of signal quantization. Simultaneously, the quantizer always has the excellent characteristic of low data transmission, which effectively saves communication resources without sacrificing performance. Thus far, quantizer has been extensively studied on linear uncertain control systems [33], aerospace engineering [34], Euler-Lagrange systems [35] and multiagent systems [36].

Motivated by the previous research, a practical fixed-time trajectory tracking control scheme is developed for the first time for underactuated AUVs with uncertain dynamics, unknown time-varying disturbances, an unknown dead zone, actuator faults and input quantization. The distinct features in this article are summarized as follows.

- Differing from the [37] and [38], this article introduces a novel nonlinear decomposition method based on quantized input signals, ensuring bounded estimation. This breakthrough addresses the conventional sector bounded quantizer's limitations related to the boundedness conditions for disturbance-like elements.
- Unlike the reference [39], our work allows for the quantization parameter can be set to any value within the interval (0, 1) without imposing additional constraints. In addition, the adaptive NN quantization control law proposed in this article is in sharp contrast to the requirements of references [40] and [41],which does not require any parameter information from the quantizer.

This article is organized as follows. The Section II introduces the mathematical model of AUVs, the problem formulation, some preliminaries and the introduction of neural network. Section III proposes the details of control law design process. The simulation results are provided in Section IV. Section V concludes this article.

Notations: In this article, $\|\bullet\|$ represents the 2-norm of a matrix or vector. Notate $\Omega^{\Lambda} = [\Omega_1{}^{\Lambda}, \cdots, \Omega_n{}^{\Lambda}]^T$, where $\Omega = [\Omega_1, \cdots, \Omega_n]^T$ denote a vector and Λ is a positive constant. $\lambda_{\max}(\bullet)$ and $\lambda_{\min}(\bullet)$ denote the maximum and the minimum eigenvalues of a matrix, respectively. $diag(\bullet)$ denotes the diagonal matrix. $\tilde{\bullet} = \bullet - \hat{\bullet}$ stands for the error between the unknown parameter • and its estimate value $\hat{\bullet}$.

II. MODEL AND PROBLEM FORMULATION

A. AUVS KINEMATIC AND DYNAMIC MODELS

In practical scenarios, only 3-DOF are relevant when considering motion control of an underactuated AUV in the horizontal plane, namely, surge, sway and yaw. The mathematical model of an underactuated AUV can be described as

$$\dot{x} = u\cos(\psi) - v\sin(\psi) \tag{1a}$$
$$\dot{y} = u\sin(\psi) + v\cos(\psi) \tag{1b}$$
$$\dot{\psi} = r \tag{1c}$$

$$m_{11}\dot{u} = f_u + \tau_u + d_{eu} \tag{2a}$$
$$m_{22}\dot{v} = f_v + d_{ev} \tag{2b}$$
$$m_{33}\dot{r} = f_r + \tau_r + d_{er} \tag{2c}$$

with

$$f_u = m_{22}vr - m_{33}wq - d_{11}u \tag{3a}$$
$$f_v = -m_{11}ur - d_{22}v \tag{3b}$$
$$f_r = (m_{11} - m_{22})uv - d_{33}r \tag{3c}$$

where x, y and ψ denote the AUV's surge position, the sway position, and the yaw angle in the earth-fixed frame, respectively. u, v and r are the surge velocity, the sway velocity and the yaw velocity of AUVs in the body-fixed frame, respectively. τ_u and τ_r are the surge control force and the yaw control moment, respectively. d_{eu}, d_{ev} and d_{er} are the time-varying environmental disturbances. m_{11}, m_{22} and m_{33} represent the inertia including added mass of AUVs. The d_{11}, d_{22} and d_{33} are hydrodynamic damping parameters.

Assumption 1: The model parameter m_{ii} and d_{ii} ($i = 1, 2, 3$) are uncertain [42].

Assumption 2: The environmental disturbance d_{en} ($n = u, v, r$) is bounded, i.e., $|d_{en}| \leq \bar{d}_{en}$ with $\bar{d}_{en}$ being an unknown positive constant [43], [44].

Assumption 3: The reference trajectory signal $\eta_d = [x_d, \ y_d]^T$ and its first two derivatives are available [44], [45].

Assumption 4: The sway velocity v of the AUVs is passive bounded [43].

Remark 1: The marine environmental disturbance operating on the AUVs is difficult to identify, and it is bounded due to its limited energy. The model parameters $m_{(\bullet)}$ and $d_{(\bullet)}$ include the added masses and inertia as well as hydrodynamic damping coefficients, which are related to marine environmental and operating conditions as well as the AUV's own characteristics. Therefore, it is difficult to obtain accurate information on these parameters. For the purpose of facilitate the design of control law, the reference trajectory in Assumption 3 is usually required to be uniform and smooth, which is a general requirement. In practice, the hydrodynamic damping force in equation (2b) dominates in the sway direction, which leads to the sway velocity is easily damped. Hence, the Assumption 4 is logical. Thus, Assumptions 1-4 are reasonable.

Lemma 1: [46]. If there have some variables $p > 0$, $q > 0$, $0 < g_2 < 1$, $g_1 > 1$ and $0 < \theta < \infty$ and there exsit Lyapunov function $V(h)$ can be expressed as

$$\dot{V}(h) \leq -pV^{g_1}(h) - qV^{g_2}(h) + \theta \tag{4}$$

Then, the origin $h = 0$ of the nonlinear system (4) is practically fixed-time stable. $V(h)$ settles within the residual set $\Omega \in \{ h : V(h) \leqslant \min\{[\frac{\theta}{p(1-\Im)}]^{\frac{1}{g_1}}, [\frac{\theta}{q(1-\Im)}]^{\frac{1}{g_2}} \}$ with $0 < \Im < 1$. The setting time $T(h_0)$ can being bound by $T(h_0) \leqslant \frac{1}{p\Im(1-g_2)} + \frac{1}{q\Im(g_1-1)}$.

Lemma 2: [47]. For any scalar ℓ and any positive constant $\partial \in R$, the following inequality holds.

$$0 < |\partial| - \frac{\partial^2}{\sqrt{\partial^2 + \ell^2}} < \ell \tag{5}$$

Lemma 3: [48]. For any $\Delta > 0$ and $N \in R$, The hyperbolic tangent function tanh() has the following properties

$$0 < |N| - N\tanh(\frac{N}{\Delta}) < 0.2785\Delta \tag{6}$$

Definition 1: By introducing the Radial Basis Function (RBF) NN to approximate an unknown continuous function $f(X)$, we have the following equation [49], [50]

$$f(X) = \omega^{*T}\varphi(X) + \kappa \tag{7a}$$
$$\varphi(X) = exp(-(X - c_j)^T(X - c_j)/b_j^2), j = 1, \ldots n \tag{7b}$$

where ω^* is the optimal weights. $\varphi(X)$ is the basis function vector. c_j and b_j are the center and the width of the Gaussian function. n is the node number of the RBF NN. The inherent approximation error κ is bounded, there exists a positive constant $\bar{\kappa}$ satisfies that $|\kappa| \leqslant \bar{\kappa}$.

B. COORDINATE TRANSFORMATION

To solve the underactuated problem of AUVs, the following coordinate transformation is introduced

$$\begin{cases} x_1 &= x + l\cos(\psi) \\ y_1 &= y + l\sin(\psi) \end{cases} \tag{8}$$

where ł is a small positive constant.

Notate $\eta_1 = [x_1, \ y_1]^T$, taking the second-order time derivative of η_1 along (2) and (3) yield

$$\ddot{\eta}_1 = R(\psi)W\tau + F + \varsigma \tag{9}$$

where $R(\varphi) = \begin{bmatrix} \cos\psi & -\sin\psi \\ \sin\psi & \cos\psi \end{bmatrix}$, $W = \begin{bmatrix} \frac{1}{m_{11}} & 0 \\ 0 & -\frac{l}{m_{33}} \end{bmatrix}$, $\tau = [\tau_u, \tau_r]^T$, $F = [F_1, F_2]^T$, $\varsigma = [\varsigma_1, \varsigma_2]^T$. Herein, $F_1 = f_u\cos(\psi) - (f_v + lf_r\sin(\psi)) + ur\sin(\psi) + (vr + lr^2)\cos(\psi)$, $F_2 = f_u\sin(\psi) - (f_v + lf_r)\cos(\psi) + ur\cos(\psi) + (vr + lr^2)\sin(\psi)$, $\varsigma_1 = \frac{d_{eu}}{m_{11}}\cos(\psi) - (\frac{d_{ev}}{m_{11}} + \frac{ld_{er}}{m_{33}})\sin(\psi)$, $\varsigma_2 = \frac{d_{eu}}{m_{11}}\sin(\psi) + (\frac{d_{ev}}{m_{11}} + \frac{ld_{er}}{m_{33}})\cos(\psi)$.

In practical engineering applications, the effectiveness of the actuator may be diminished. These actuator faults can be described uniformly as follows

$$\tau = \gamma \tau^f + \chi \tag{10}$$

where $\tau = [\tau_u{}^f, \tau_r{}^f]^T$ $(\varepsilon = u, r)$ is the control input signal for the control law design, $\gamma = diag(\gamma_u, \gamma_r)$ is the unknown time-varying parameter vector $0 < \gamma_\varepsilon < 1$, $\chi(t) = [\chi_u, \chi_r]^{\mathrm{T}}$ denotes an unknown bounded vector.

Remark 2: Actuator faults consist of LOE, bias, and lock-in-place (LIP) faults. LOE fault is attributed to mechanical wear, aging. In other word, $0 < \gamma_\varepsilon < 1$ means that the actuator suffers from LOE fault. Bias fault is attributed to installation displacement or other mechanical factors. It is worth emphasizing that in the above equation describing an actuator fault, both LOE and bias faults are present in the system. If the actuator suffer from a LIP fault, $\tau^f = \bar{\tau}^f$ for all $\forall t \geqslant t^f$. Because of the underactuated nature, this article ignores LIP fault in the control law design to guarantee the controllability of AUVs.

The control input signal in this article under the influence of dead zone nonlinearity can be depicted as follows

$$\tau_\varepsilon{}^f = H(J_\varepsilon(t)) = \begin{cases} a_\varepsilon(J_\varepsilon - b_{\mathcal{A},\varepsilon}), & J_\varepsilon \geqslant b_{\mathcal{A},\varepsilon} \\ 0, & b_{\mathcal{P},\varepsilon} < J_\varepsilon < b_{\mathcal{A},\varepsilon} \\ a_\varepsilon(J_\varepsilon - b_{\mathcal{P},\varepsilon}), & J_\varepsilon \leqslant b_{\mathcal{P},\varepsilon} \end{cases} \tag{11}$$

Further, the equation (11) can be rewritten as

$$H(J_\varepsilon(t)) = a_\varepsilon J_\varepsilon + L_\varepsilon \tag{12}$$

with

$$L = \begin{cases} -a_\varepsilon b_{\mathcal{A},\varepsilon}, & J_\varepsilon \geqslant b_{\mathcal{A},\varepsilon} \\ -a_\varepsilon J_\varepsilon, & b_{\mathcal{P},\varepsilon} < J_\varepsilon < b_{\mathcal{A},\varepsilon} \\ -a_\varepsilon b_{\mathcal{P},\varepsilon}, & J_\varepsilon \leqslant b_{\mathcal{P},\varepsilon} \end{cases} \tag{13}$$

where $J_\varepsilon(t)$ is the dead zone input. $a_\varepsilon > 0$, $b_{\mathcal{A},\varepsilon}$ and $b_{\mathcal{P},\varepsilon}$ are the unknown dead zone parameters. Here $a = \mathrm{diag}(a_u, a_r)$, $J = [J_u, J_r]^{\mathrm{T}}, L = [L_u, L_r]^{\mathrm{T}}$.

Here, the dead zone vector a is bounded. From (13), it can be seen that

$$\|L\| \leq L^* \tag{14}$$

where $L^* = \max\{a_{\varepsilon\max} b_{\mathcal{A},\varepsilon\max}, -a_{\varepsilon\max} b_{\mathcal{P},\varepsilon\min}\}$, $b_{\mathcal{P},\varepsilon\min}$ is the lower bound of $b_{\mathcal{P},\varepsilon}$. $a_{\varepsilon\max}$ and $b_{\mathcal{A},\varepsilon\max}$ are the upper bound of parameter a_ε and $b_{\mathcal{A},\varepsilon}$, respectively.

Furthermore, the dead zone input can be expressed as $J_\varepsilon = Q(\mu_\varepsilon)$. It should be note that $Q(\mu_\varepsilon)$ indicates the quantified value. The hysteresis quantizer is introduced in this article as in (15), as shown at the bottom of the page.

In (15), $\mu_{\varepsilon i} = \rho^{(1-i)}\mu_{\varepsilon i\min}$, $(i = 1, 2 \cdots)$. $\mu_{\varepsilon i\min} > 0$ is the dead zone parameter of the quantizer. δ_ε is a positive parameter and satisfies $0 < \delta_\varepsilon < 1$. $0 < \rho < 1$ is the quantized density and $\rho = \frac{1-\delta_\varepsilon}{1+\delta_\varepsilon}$. $Q(\mu_\varepsilon)$ is in the set $(0, \pm\mu_\varepsilon{}^{(i)}, \pm\mu_\varepsilon{}^{(i)}(1+\delta_\varepsilon)$. The detailed information about its parameters and the hysteresis quantizer can be found in the work [51].

On the basis of the nonlinear decomposition introduced for the quantized signal. Hence, the quantizer $Q(\mu_\varepsilon)$ can be described as the following form:

$$Q(\mu_\varepsilon) = G_\varepsilon \mu_\varepsilon(t) + \lambda_\varepsilon \tag{16}$$

where $\mu = [\mu_u, \mu_r]^T$, $G = diag(G_u, G_r)$, $\lambda = [\lambda_u, \lambda_r]^T$.

Remark 3: The conventional linear decomposition $Q(\mu_\varepsilon) = \mu_\varepsilon + \lambda_\varepsilon$ is used in the conventional sector bounded quantizer, while the assumption of boundedness of the disturbances-like term λ_ε is required. It is challenging to demonstrate the boundedness of the disturbances-like term λ_ε for control design, as it does not satisfy certain conditions $\lambda_\varepsilon \leqslant |\delta\mu_\varepsilon|$. To overcome this limitation, a new nonlinear decomposition (16) of the quantized input is introduced in this approach. By utilizing this nonlinear decomposition, the design difficulty regarding the boundedness of the disturbances-like term λ_ε is resolved, allowing the application of conventional analysis tools such as fuzzy control theory to study the quantization effect. Consequently, the restrictive conditions imposed on the disturbances-like term λ_ε in references [52] and [53] can be eliminated. Similar analyses can be found in references [54] and [55].

By letting $\dot{\eta}_1 = \eta_2$, we have

$$\dot{\eta}_1 = \eta_2 \tag{17}$$

$$\dot{\eta}_2 = RW\gamma G\mu + F + RW(\gamma a\lambda + \gamma L + \chi) + \varsigma \tag{18}$$

Remark 4: As we mentioned above, l is a positive constant. $\|R(\psi)\| = 1$, $W\gamma G$ is a nonsingular control gain matrix, we can effectively handle the underactuation problem of AUVs by the coordinate transformation (8). Further, the positive constant l impacts the tracking accuracy of AUVs. As $l \to 0$, the $x_1 \to x$ and $y_1 \to y$, it means that the smaller l is, the higher tracking control accuracy can be obtained.

In this article, the main objective is to conceive the fixed-time trajectory tracking control scheme for underactuated AUVs satisfying Assumptions 1-4 suffering from uncertain dynamics, environmental disturbances, an unknown dead zone, actuator faults and input quantization such that tracking errors can converge to a small residual set within fixed time.

$$Q(\mu_{\varepsilon i}) = \begin{cases} \mu_{\varepsilon i} sign(\mu_\varepsilon) & \frac{\mu_{\varepsilon i}}{1+\delta_\varepsilon} < |\mu_\varepsilon| \leq \mu_{\varepsilon i}, \quad \dot{\mu}_\varepsilon < 0, \quad or \quad \mu_{\varepsilon i} < |\mu_\varepsilon| \leq \frac{\mu_{\varepsilon i}}{1-\delta_\varepsilon}, \quad \dot{\mu}_\varepsilon > 0 \\ \mu_{\varepsilon i}(1+\delta_\varepsilon) sign(\mu_\varepsilon) & \mu_{\varepsilon i} < |\mu_\varepsilon| \leq \frac{\mu_{\varepsilon i}}{1-\delta_\varepsilon}, \quad \dot{\mu}_\varepsilon < 0, \quad or \quad \frac{\mu_{\varepsilon i}}{1-\delta_\varepsilon} < |\mu_\varepsilon| \leq \frac{\mu_{\varepsilon i}(1+\delta_\varepsilon)}{1-\delta_\varepsilon}, \quad \dot{\mu}_\varepsilon > 0 \\ 0 & 0 < |\mu_\varepsilon| \leq \frac{\mu_{\varepsilon\min}}{1+\delta_\varepsilon}, \quad \dot{\mu}_\varepsilon < 0, \quad or \quad \frac{\mu_{\varepsilon\min}}{1+\delta_\varepsilon} < |\mu_\varepsilon| \leq \mu_{\varepsilon\min}, \quad \dot{\mu}_\varepsilon > 0 \\ q(\mu_\varepsilon(t^-)) & \dot{\mu}_\varepsilon = 0 \end{cases} \tag{15}$$

III. CONTROL LAW DESIGN AND STABILITY ANALYSIS

First, we can define the error variables $s_1 = [s_{11},\ s_{12}]^T \in R^2$ and $s_2 = [s_{21},\ s_{22}]^T \in R^2$ as below

$$s_1 = \eta_1 - \eta_d \tag{19}$$

$$s_2 = \eta_2 - \alpha \tag{20}$$

where α is the virtual control law to be designed later.

Taking the time derivative of s_1, we have

$$\dot{s}_1 = s_2 + \alpha - \dot{\eta}_d \tag{21}$$

To proceed, the virtual control law can be designed as

$$\alpha = -k_{11}\frac{s_1}{\sqrt{\|s_1\|^2+\iota^2}} - k_{12}{s_1}^3 + \dot{\eta}_d \tag{22}$$

where $k_{11} \in R^{2\times 2}$ and $k_{12} \in R^{2\times 2}$ are positive-definite design matrices, and ι is a positive parameter.

Therefore, (22) can be rewritten as

$$\dot{s}_1 = s_2 - k_{11}\frac{s_1}{\sqrt{\|s_1\|^2+\iota^2}} - k_{12}{s_1}^3 \tag{23}$$

According to (18) and (20), taking the time derivative of (20) yields

$$\dot{s}_2 = RW\gamma G\mu + RW(\gamma a\lambda\!\!\!- + \gamma L + \chi) + \varsigma + F - \dot{\alpha} \tag{24}$$

Notate $\|W\gamma G\|$ is bounded. Herein, let $\wp = W\gamma G$ and $\xi = \wp^{-1}$.

In this article, the RBF NN is introduced to approximate the uncertain term $RW(\gamma a\lambda + \gamma L + \chi) + F - \dot{\alpha} = {\omega^*}^{\mathrm{T}}\phi(\Im) + \varpi$. Herein, $\omega^* = [\omega_1^{*\mathrm{T}}\ \ 0_{1\times n}; 0_{1\times n}\ \ \omega_1^{*\mathrm{T}}]$ is the ideal weight matrix with $\omega_i^* = [\omega_{i,1}^*, \cdots, \omega_{i,n}^*]^{\mathrm{T}}$ $(i = 1, 2)$, n denotes the node number of the RBF NN. $\phi(\Im) = [\phi_1^{\mathrm{T}}(\Im), \phi_2^{\mathrm{T}}(\Im)]^{\mathrm{T}}$ represents the basis function vector with $\phi_i(\Im) = [\phi_{i,1}(\Im), \cdots, \phi_{i,n}(\Im)]^{\mathrm{T}}$. ϖ is the NN approximation error. We can obtain that $\|\omega^*\| \leqslant \omega_m$ and $\|\varpi\| \leqslant \varpi_m$ are bound, where ω_m and ϖ_m represent unknown positive constants. Meanwhile, adaptive control technique is introduced to estimate the upper bounds of the disturbances ς, and parameter adaptive technique is used to estimate the parameter ξ.

Design the control law as

$$\mu = -R^T\frac{s_2\hat{\xi}^T\hat{\xi}\beta^T\beta}{\sqrt{\hat{\xi}^T\hat{\xi}{s_2}^T s_2\beta^T\beta+\iota}} \tag{25}$$

$$\beta = k_{21}\frac{s_2}{\sqrt{\|s_2\|^2+\iota^2}} + k_{22}{s_2}^3 + \hat{\omega}^T\phi + \hat{h}\tanh(\frac{s_2}{\aleph}) \tag{26}$$

with adaptive laws

$$\dot{\hat{\omega}} = \Gamma(\phi {s_2}^T - \sigma_1\hat{\omega} - \sigma_2\hat{\omega}^3) \tag{27}$$

$$\dot{\hat{\xi}} = H(\beta {s_2}^T - \Xi_1\hat{\xi} - \Xi_2\hat{\xi}^3) \tag{28}$$

$$\dot{\hat{h}} = \Phi(\tanh(\frac{s_2}{\aleph}){s_2}^T - \vartheta_1\hat{h} - \vartheta_2\hat{h}^3) \tag{29}$$

where $\Gamma = \Gamma^T$ is a diagonal matrix, $\sigma_1, \sigma_2, k_{21}, k_{22}, H, \Xi_1, \Xi_2, \Phi, \aleph, \vartheta_1$ and ϑ_2 positive-definite design matrices. $\hat{\omega}$, $\hat{\xi}$ and $\hat{h}$ are the estimate of ω^*, ξ and h, respectively.

Remark 5: Compared with [39], the quantization parameter δ_ε in this article can be chosen as any scalar in the range (0, 1) without need to satisfy any constraints, and the closed-loop system still maintains improved stability and robustness. The length of the quantization interval is defined as ℓ, and the hysteresis width constant $\hbar = p_\hbar\ell$ should be satisfied with $0 < p_\hbar \leqslant 0.5$ in [39]. Different from [40] and [41], the neural adaptive quantization control law proposed in this article does not require any parameter information of the quantizer because of the quantizer parameters do not need to be injected into the control law.

Theorem 1: Applying the hysteresis quantizer (15), the virtual control law (22), the adaptive laws (27), (28), (29), the design control law (25) and (26) to the AUVs trajectory tracking system (1a)-(1b), (2a)-(2b) and (3a)-(3b) with uncertain dynamics, time-varying disturbances, an unknown dead zone, actuator faults and input quantization under Assumptions 1-4. Tracking errors can converge to the neighborhood of zero within fixed time. All the signal in AUVs trajectory tracking closed-loop system are uniformly ultimately bounded.

Proof: The Lyapunov function can be selected as

$$V = \frac{1}{2}{s_1}^T s_1 + \frac{1}{2}{s_2}^T s_2 + \frac{1}{2}\tilde{\omega}^T\Gamma^{-1}\tilde{\omega} + \frac{1}{2}\tilde{\xi}^T H^{-1}\wp\tilde{\xi} + \frac{1}{2}\tilde{h}^T\Phi^{-1}\tilde{h} \tag{30}$$

The time derivative of (30) can be obtained

$$\dot{V} = {s_1}^T\dot{s}_1 + {s_2}^T\dot{s}_2 + \tilde{\omega}^T\Gamma^{-1}\dot{\tilde{\omega}} + \tilde{\xi}^T H^{-1}\wp\dot{\tilde{\xi}} + \tilde{h}^T\Phi^{-1}\dot{\tilde{h}} \tag{31}$$

According to (23), we have

$${s_1}^T\dot{s}_1 = {s_1}^T s_2 - \frac{{s_1}^T k_{11}s_1}{\sqrt{\|s_1\|^2+\iota^2}} - {s_1}^T k_{12}{s_1}^3 \tag{32}$$

Combining Lemma 2 and (32), we have

$$-\frac{{s_2}^T\wp s_2\hat{\xi}^T\hat{\xi}\beta^T\beta}{\sqrt{\hat{\xi}^T\hat{\xi}{s_2}^T s_2\beta^T\beta+\iota}} \leq \|\wp\|\sqrt{\iota} - \beta^T\wp\hat{\xi}s_2 \tag{33}$$

According to (24)-(26) and (33), we have

$$\begin{aligned}
{s_2}^T\dot{s}_2 &\leq \|\wp\|\sqrt{\iota} - \beta^T\wp\hat{\xi}s_2 + s_2\beta - s_2\beta \\
&\quad + {s_2}^T[RW(\gamma a\lambda\!\!\!- + \gamma L + \chi) + \varsigma + {\omega^*}^T\phi + \varpi] \\
&\leq \|\wp\|\sqrt{\iota} - \beta^T\wp\hat{\xi}s_2 + s_2\beta - \frac{{s_2}^T k_{21}s_2}{\sqrt{\|s_2\|^2+\iota^2}} \\
&\quad - {s_2}^T k_{22}{s_2}^3 - {s_2}^T\hat{h}\tanh(\frac{s_2}{\aleph}) + {s_2}^T h \\
&\quad + {s_2}^T\tilde{\omega}^T\phi + {s_2}^T\varpi \\
&\leq \|\wp\|\sqrt{\iota} - \beta^T\wp\hat{\xi}s_2 + s_2\beta - \frac{{s_2}^T k_{21}s_2}{\sqrt{\|s_2\|^2+\iota^2}} \\
&\quad - {s_2}^T k_{22}{s_2}^3 + {s_2}^T\tilde{h}\tanh(\frac{s_2}{\aleph}) + 0.2785\,\|h\|\,\aleph \\
&\quad + {s_2}^T\tilde{\omega}^T\phi + {s_2}^T\varpi
\end{aligned} \tag{34}$$

According to (27)-(29), we have

$$\tilde{\omega}\Gamma^{-1}\dot{\hat{\omega}} = -\tilde{\omega}(\phi {s_2}^T - \sigma_1\hat{\omega} - \sigma_2\hat{\omega}^3) \tag{35}$$

$$\tilde{\xi}H^{-1}\wp\dot{\hat{\xi}} = -\tilde{\xi}\wp({s_2}^T\beta - \Xi_1\hat{\xi} - \Xi_2\hat{\xi}^3) \tag{36}$$

$$\tilde{h}\Phi^{-1}\dot{\hat{h}} = -\tilde{h}({s_2}^T\tanh(\frac{s_2}{\aleph}) - \vartheta_1\hat{h} - \vartheta_2\hat{h}^3) \tag{37}$$

By virtue of (31)-(37), we have

$$\begin{aligned}\dot{V} &= {s_1}^T s_2 - k_{11}\frac{{s_1}^T s_1}{\sqrt{\|s_1\|^2+\iota^2}} - {s_1}^T k_{12}{s_1}^3 \\ &+ \|\wp\|\sqrt{\iota} - \frac{{s_2}^T k_{21}s_2}{\sqrt{\|s_2\|^2+\iota^2}} - {s_2}^T k_{22}{s_2}^3 \\ &+ 0.2785\,\|h\|\,\aleph + {s_2}^T\varpi + \tilde{\omega}^T\sigma_1\hat{\omega} + \tilde{\omega}^T\sigma_2\hat{\omega}^3 \\ &+ \tilde{\xi}^T\wp\Xi_1\hat{\xi} + \tilde{\xi}^T\wp\Xi_2\hat{\xi}^3 + \tilde{h}^T\vartheta_1\hat{h} + \tilde{h}^T\vartheta_2\hat{h}^3\end{aligned} \tag{38}$$

In the light of Young's inequality, we can obtain

$$\begin{aligned}\tilde{\omega}^T\sigma_1\hat{\omega} &= (\frac{1}{2}\tilde{\omega}^T\sigma_1\tilde{\omega})^{\frac{1}{2}} - (\frac{1}{2}\tilde{\omega}^T\sigma_1\tilde{\omega})^{\frac{1}{2}} + \tilde{\omega}^T\sigma_1\hat{\omega} \\ &\le \frac{1}{4} + \frac{1}{2}\tilde{\omega}^T\sigma_1\tilde{\omega} - (\frac{1}{2}\tilde{\omega}^T\sigma_1\tilde{\omega})^{\frac{1}{2}} \\ &\quad + \frac{1}{2}\omega^{*T}\sigma_1\omega^* - \frac{1}{2}\tilde{\omega}^T\sigma_1\tilde{\omega} \\ &\le -(\frac{1}{2}\tilde{\omega}^T\sigma_1\tilde{\omega})^{\frac{1}{2}} + \frac{1}{2}\omega^{*T}\sigma_1\omega^* + \frac{1}{4}\end{aligned} \tag{39}$$

$$\begin{aligned}\tilde{\xi}^T\wp\Xi_1\hat{\xi} &= (\frac{1}{2}\tilde{\xi}^T\wp\Xi_1\tilde{\xi})^{\frac{1}{2}} - (\frac{1}{2}\tilde{\xi}^T\wp\Xi_1\tilde{\xi})^{\frac{1}{2}} + \tilde{\xi}^T\wp\Xi_1\hat{\xi} \\ &\le \frac{1}{4} + \frac{1}{2}\tilde{\xi}^T\wp\Xi_1\tilde{\xi} - (\frac{1}{2}\tilde{\xi}^T\wp\Xi_1\tilde{\xi})^{\frac{1}{2}} \\ &\quad + \frac{1}{2}\xi^T\wp\Xi_1\xi - \frac{1}{2}\tilde{\xi}^T\wp\Xi_1\tilde{\xi} \\ &\le -(\frac{1}{2}\tilde{\xi}^T\wp\Xi_1\tilde{\xi})^{\frac{1}{2}} + \frac{1}{2}\xi^T\wp\Xi_1\xi + \frac{1}{4}\end{aligned} \tag{40}$$

$$\begin{aligned}\tilde{h}^T\vartheta_1\hat{h} &= (\frac{1}{2}\tilde{h}^T\vartheta_1\tilde{h})^{\frac{1}{2}} - (\frac{1}{2}\tilde{h}^T\vartheta_1\tilde{h})^{\frac{1}{2}} + \tilde{h}^T\vartheta_1\hat{h} \\ &\le \frac{1}{4} + \frac{1}{2}\tilde{h}^T\vartheta_1\tilde{h} - (\frac{1}{2}\tilde{h}^T\vartheta_1\tilde{h})^{\frac{1}{2}} + \frac{1}{2}h^T\vartheta_1 h - \frac{1}{2}\tilde{h}^T\vartheta_1\tilde{h} \\ &\le -(\frac{1}{2}\tilde{h}^T\vartheta_1\tilde{h})^{\frac{1}{2}} + \frac{1}{2}h^T\vartheta_1 h + \frac{1}{4}\end{aligned} \tag{41}$$

We know that the following equation holds

$$\begin{aligned}\tilde{\omega}^T\sigma_2\hat{\omega}^3 &= \tilde{\omega}^T\sigma_2\omega^{*3} - 3\tilde{\omega}^T\sigma_2\tilde{\omega}\omega^{*T}\omega^* \\ &\quad + 3\omega^{*T}\sigma_2\tilde{\omega}^3 - \tilde{\omega}^T\sigma_2\tilde{\omega}^3\end{aligned} \tag{42}$$

According to Young's inequality, we have

$$\tilde{\omega}^T\sigma_2\omega^{*3} \le 3\tilde{\omega}^T\sigma_2\tilde{\omega}\omega^{*T}\omega + \frac{1}{4}\omega^{*T}\sigma_2\omega^{*3} \tag{43}$$

$$3\omega^{*T}\sigma_2\tilde{\omega}^3 \le \frac{9}{4}\nu^{\frac{4}{3}}\tilde{\omega}^T\sigma_2\tilde{\omega}^3 + \frac{3}{4\nu^4}\omega^{*T}\sigma_2\omega^{*3} \tag{44}$$

Substituting (43)-(44) into (42) yield

$$\tilde{\omega}^T\sigma_2\hat{\omega}^3 \le -\tilde{\omega}^T(\sigma_2 - \frac{9}{4}\nu^{\frac{4}{3}}I)\tilde{\omega}^3 + \omega^{*T}(\frac{1}{4}\sigma_2 + \frac{3}{4\nu^4}I)\omega^{*3} \tag{45}$$

Similar to (42)-(45), we have

$$\tilde{\xi}^T\wp\Xi_2\hat{\xi}^3 \le -\tilde{\xi}^T(\wp\Xi_2 - \frac{9}{4}\nu^{\frac{4}{3}}I)\tilde{\xi}^3 + \xi^T(\frac{1}{4}\wp\Xi_2 + \frac{3}{4\nu^4}I)\xi^3 \tag{46}$$

$$\tilde{h}^T\vartheta_2\hat{h}^3 \le -\tilde{h}^T(\vartheta_2 - \frac{9}{4}\nu^{\frac{4}{3}}I)\tilde{h}^3 + h^T(\frac{1}{4}\vartheta_2 + \frac{3}{4\nu^4}I)h^3 \tag{47}$$

Synthesizing (38)-(47), we can obtain that

$$\begin{aligned}\dot{V} &\le -\frac{{s_1}^T k_{11}s_1}{\sqrt{\|s_1\|^2+\iota^2}} - {s_1}^T(k_{12} - \frac{1}{4}I){s_1}^3 + \|\wp\|\sqrt{\iota} \\ &- \frac{{s_2}^T k_{21}s_2}{\sqrt{\|s_2\|^2+\iota^2}} - {s_2}^T(k_{22} - \frac{1}{2}I){s_2}^3 - (\frac{1}{2}\tilde{\omega}^T\sigma_1\tilde{\omega})^{\frac{1}{2}} \\ &- \tilde{\omega}^T(\sigma_2 - \frac{9}{4}\nu^{\frac{4}{3}}I)\tilde{\omega}^3 - (\frac{1}{2}\tilde{\xi}^T\wp\Xi_1\tilde{\xi})^{\frac{1}{2}} - (\frac{1}{2}\tilde{h}^T\vartheta_1\tilde{h})^{\frac{1}{2}} \\ &- \tilde{\xi}^T(\wp\Xi_2 - \frac{9}{4}\nu^{\frac{4}{3}}I)\tilde{\xi}^3 - \tilde{h}^T(\vartheta_2 - \frac{9}{4}\nu^{\frac{4}{3}}I)\tilde{h}^3 \\ &+ 0.2785\,\|h\|\,\aleph + \frac{1}{4}{\varpi_m}^4 + \frac{1}{2}\omega^{*T}\sigma_1\omega^* + \frac{7}{4} \\ &+ \omega^{*T}(\frac{1}{4}\sigma_2 + \frac{3}{4\nu^4}I)\omega^{*3} + \frac{1}{2}\xi^T\wp\Xi_1\xi + \frac{1}{2}h^T\vartheta_1 h \\ &+ \xi^T(\frac{1}{4}\wp\Xi_2 + \frac{3}{4\nu^4}I)\xi^3 + h^T(\frac{1}{4}\vartheta_2 + \frac{3}{4\nu^4}I)h^3\end{aligned} \tag{48}$$

By virtue of Lemma 2, we have

$$\begin{aligned}\dot{V} &\le -\lambda_{\min}(k_{11})\,\|s_1\| - {s_1}^T(k_{12} - \frac{1}{4}I){s_1}^3 - \lambda_{\min}(k_{21})\,\|s_2\| \\ &- {s_2}^T(k_{22} - \frac{1}{2}I){s_2}^3 - (\frac{1}{2}\tilde{\omega}^T\sigma_1\tilde{\omega})^{\frac{1}{2}} - \tilde{\omega}^T(\sigma_2 - \frac{9}{4}\nu^{\frac{4}{3}}I)\tilde{\omega}^3 \\ &- (\frac{1}{2}\tilde{\xi}^T\wp\Xi_1\tilde{\xi})^{\frac{1}{2}} - \tilde{\xi}^T(\wp\Xi_2 - \frac{9}{4}\nu^{\frac{4}{3}}I)\tilde{\xi}^3 - (\frac{1}{2}\tilde{h}^T\vartheta_1\tilde{h})^{\frac{1}{2}} \\ &- \tilde{h}^T(\vartheta_2 - \frac{9}{4}\nu^{\frac{4}{3}}I)\tilde{h}^3 + 2\iota + \|\wp\|\sqrt{\iota} + 0.2785\,\|h\|\,\aleph \\ &+ \frac{1}{4}{\varpi_m}^4 + \frac{1}{2}\omega^{*T}\sigma_1\omega^* + \frac{7}{4} + \omega^{*T}(\frac{1}{4}\sigma_2 + \frac{3}{4\nu^4}I)\omega^{*3} \\ &+ \frac{1}{2}\xi^T\wp\Xi_1\xi + \xi^T(\frac{1}{4}\wp\Xi_2 + \frac{3}{4\nu^4}I)\xi^3 + \frac{1}{2}h^T\vartheta_1 h \\ &+ h^T(\frac{1}{4}\vartheta_2 + \frac{3}{4\nu^4}I)h^3\end{aligned} \tag{49}$$

Besides, the design parameters k_{12}, k_{22}, σ_2, Ξ_2 and ϑ_2 should satisfy

$$\lambda_{\min}(k_{12}) - 0.25 > 0 \tag{50}$$

$$\lambda_{\min}(k_{22}) - 0.5 > 0 \tag{51}$$

$$\lambda_{\min}(4\sigma_2) - 9\nu^{\frac{4}{3}} > 0 \tag{52}$$

$$\lambda_{\min}(4\Xi_2) - 9\nu^{\frac{4}{3}}\wp^{-1} > 0 \tag{53}$$

$$\lambda_{\min}(4\vartheta_2) - 9\nu^{\frac{4}{3}}\wp^{-1} > 0 \tag{54}$$

Then, we can conclude that

$$\dot{V} \le -A\|V\|^{\frac{1}{2}} - B\|V\|^2 + X \tag{55}$$

where $A = \min\{\sqrt{2}\lambda_{\min}(k_{11}), \sqrt{2}\lambda_{\min}(k_{21}), \sqrt{\lambda_{\min}(\Gamma\sigma_1)}, \sqrt{\lambda_{\min}(H\Xi_1)}, \sqrt{\lambda_{\min}(\Phi\vartheta_1)}\}$, $B = \min\{\lambda_{\min}(4k_{12} - I),$

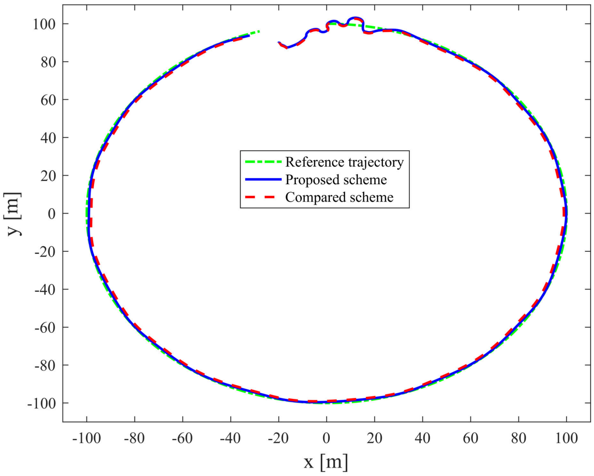

FIGURE 1. Reference and actual trajectories of the AUVs.

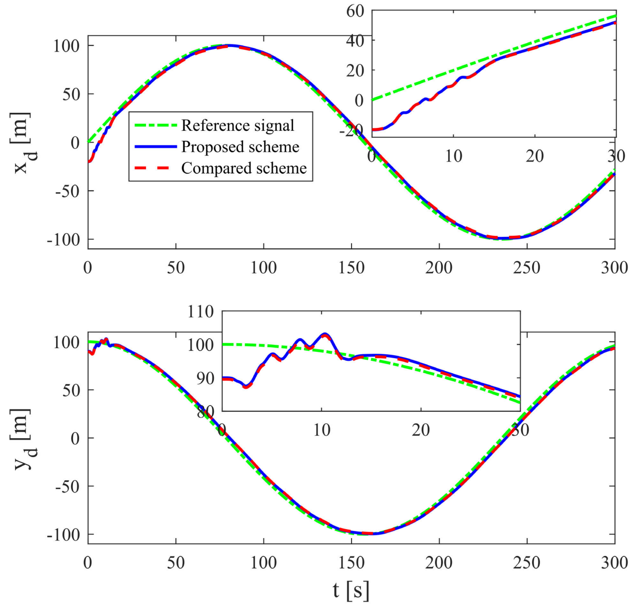

FIGURE 2. Reference and actual positions.

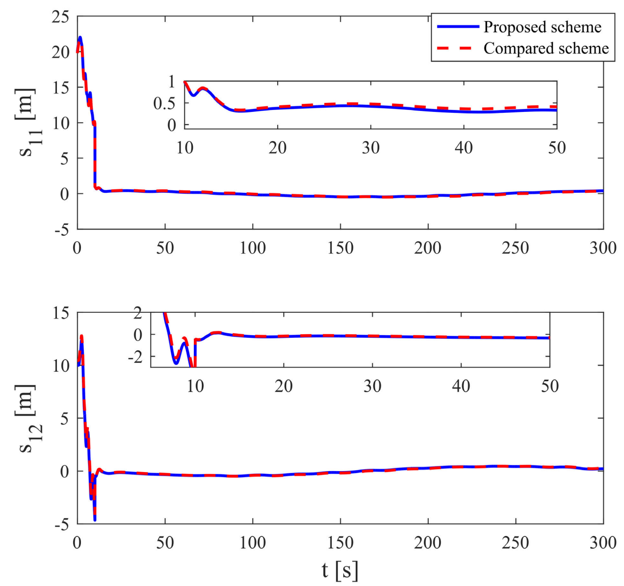

FIGURE 3. Position tracking errors.

$\lambda_{\min}(4k_{22} - 2I)$, $\lambda_{\min}(\Gamma^T(4\sigma_2 - 9\nu^{\frac{4}{3}}I)\Gamma)$, $\lambda_{\min}(H^T(4\Xi_2 - 9\nu^{\frac{4}{3}}I\wp^{-1})H)$, $\lambda_{\min}(\Phi^T(4\vartheta_2 - 9\nu^{\frac{4}{3}}I)\Phi)\}$ and $X = 2\iota + \|\wp\|\sqrt{\iota} + 0.2785\,\|h\|\,\aleph + 0.25{\varpi_m}^4 + 0.5{\omega^*}^T\sigma_1\omega^* + 1.75 + {\omega^*}^T(0.25\sigma_2 + 0.75\nu^{-4}I){\omega^*}^3 + 0.5\xi^T\wp\Xi_1\xi + \xi^T(0.25\wp\Xi_2 + 0.75\nu^{-4}I)\xi^3 + 0.5h^T\vartheta_1 h + h^T(0.25\vartheta_2 + 0.75\nu^{-4}I)h^3$.

Remark 6: In the light (30), (50) and Lemma 1, $V(h)$ could settles within the residual set $\Omega \in \{h : V(h) \leq \min\{[\frac{X}{A(1-\Im)}]^2, [\frac{X}{B(1-\Im)}]^{\frac{1}{2}}\}$, and the setting time is given by $T \leq \frac{2}{A\Im} + \frac{1}{B\Im}$. The fixed-time control schemes can convergence to a small set around the origin, and the setting time independence of the initial state. Herein, the settling time depends on the control law design parameters A and B. Here, we can decrease the settling time by increasing the design parameters A and B. Conversely, it will increase the settling time.

This concludes the proof.

IV. SIMULATION RESULTS

Simulation studies on an AUV are conducted to validate the effectiveness of proposed control scheme, whereby the main parameters are as follows: $m_{11} = 200kg$, $m_{22} = 250kg$, $m_{33} = 80kg \cdot m^2$. $d_{11} = 70kg/s$, $d_{22} = 100kg/s$, $d_{33} = 50kg/m^2s$. To demonstrate the superiority of the proposed control scheme, we refer to [56] in this article.

The time-varying external disturbances are selected as $[d_{eu}, d_{ev}, d_{er}] = [10 + 1.8\sin(0.7t) + 1.2\sin(0.9t) \quad N, 5 + 0.4\sin(0.1t) + 0.2\cos(0.6t) \quad N, 0 \quad N \cdot m]^T$. The reference trajectory is selected as $x_d = 100\sin(0.02\pi t)$, $y_d = 100\cos(0.02\pi t)$.

The initial condition is selected as $[x(0), y(0), \psi(0)] = [-20 \quad m, 90 \quad m, -0.02\pi \quad rad]^T$, $[u(0), v(0), r(0)] = [0 \quad m/s, 0 \quad m/s, 0 \quad rad/s]^T$.

Here, user-defined the parameters for control laws are as follows: $k_{11} = diag(2, 2)$, $k_{12} = diag(0.3, 0.3)$, $k_{21} = diag(6, 2)$, $k_{22} = diag(0.6, 0.6)$, $\aleph = 0.2$, $l = 0.12$, $\iota = 3$, $\Gamma = diag(120I_{64\times64}, 120I_{64\times64})^T$, $\sigma_1 = diag(0.005, 0.005)$, $\sigma_2 = diag(0.005, 0.005)$, $\Phi = diag(20, 20)$, $\vartheta_1 = diag(0.01, 0.01)$, $\vartheta_2 = diag(0.005, 0.005)$, $H = diag(18, 18)$, $\Xi_1 = diag(0.02, 0.02)$, $\Xi_2 = diag(0.1, 0.1)$. The actuator faults occur at $T = 40s$, the actuator faults parameters $\gamma = diag(\gamma_u, \gamma_r) = diag(0.7, 0.7)$, $\chi(t) = [30, 30]^T$. The dead zone parameters are selected as $a = \mathrm{diag}(1.2, 1.2)$, $b_{\mathcal{A},u} = b_{\mathcal{A},r} = 10$, $b_{\mathcal{P},u} = b_{\mathcal{P},r} = -5$. Parameters of the quantizer are selected as $\rho = 0.6666$, $i = 50$, $\tau_{u\min} = \tau_{r\min} = 5$, $\delta_u = \delta_r = 0.2$.

The simulation studies under the two control schemes are displayed in Figures 1-7. Figure 1 illustrates that the AUVs can track the reference trajectory under two control schemes.

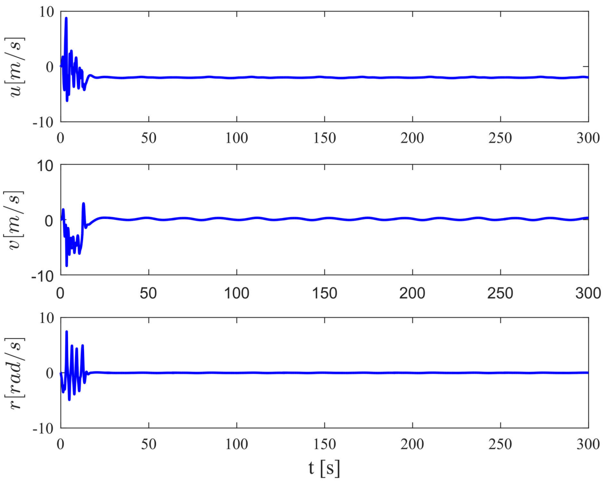

FIGURE 4. Velocities of AUVs.

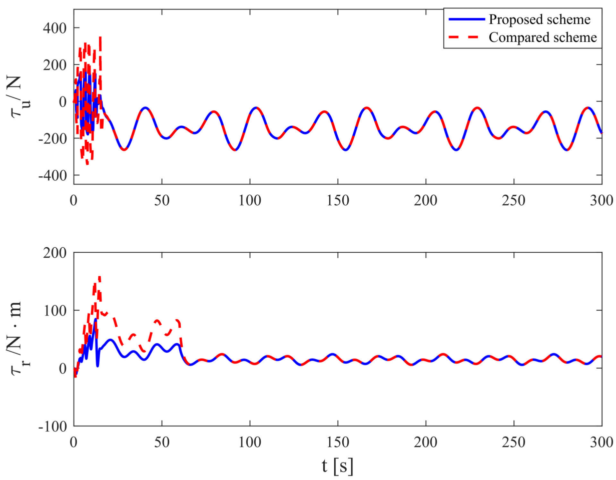

FIGURE 5. Actual control input signals τ_u and τ_r.

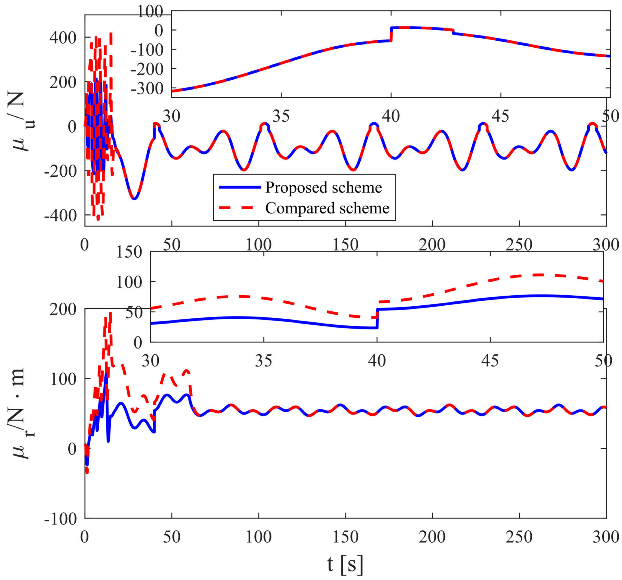

FIGURE 6. The signals to be quantized μ_u and μ_r.

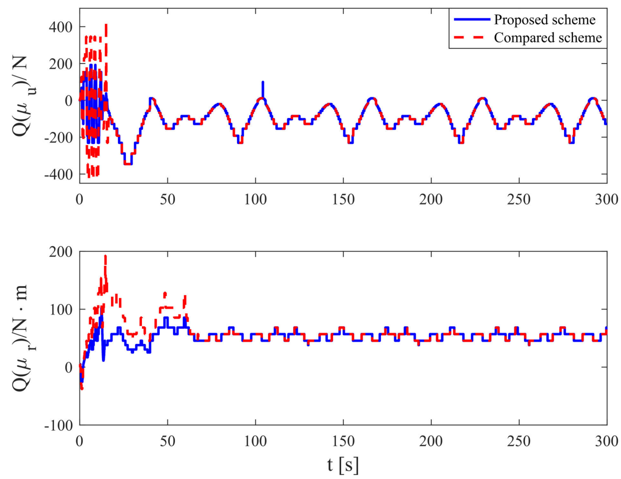

FIGURE 7. The quantified signals $Q(\mu_u)$ and $Q(\mu_r)$.

In Figure 2, it is obvious that the two control schemes can force the actual position of an underactuated AUV track the reference position. Figure 3 plot the duration curves of position tracking errors, respectively. They describes that position tracking errors are bounded under both fault-tolerant control schemes. Figure 4 portrays that the surge velocity, sway velocity vand yaw velocity of underactuated AUVs are bounded. Figure 5 depicts the actual control input signal of the AUVs trajectory tracking control systems. Figure 6 shows the signal to be quantized of the AUVs trajectory tracking control systems. It is worth noting that the signal produces a small overshoot at 40s. Figure 7 describes the quantified signal of the AUVs trajectory tracking control systems. At the start of system operation, the actual control input, the signal to be quantized and the quantized signal all exhibit large fluctuations under the compared control scheme. All the control signal under two control scheme are bounded and reasonable. Figures 5-7 indicate that there are significant fluctuations in both the signal to be quantized and the signal after quantization when the system is in the initial operating phase under the compared control scheme than proposed control scheme. Similarly, the input to the system exhibits considerable fluctuations, resulting in inadequate system stability and robustness.

V. CONCLUSION

In this article, a practical fixed-time adaptive NN quantization FTC control scheme is proposed for underactuated AUVs with uncertain dynamics, unknown environmental disturbances, an unknown dead zone and actuator faults. The error transformation is introduced to redefine the output and thus solve the underactuation problem of the AUV. Herein, a hysteresis quantizer is introduced to decrease the oscillation in the signal quantization process. To proceed, the adaptive NN to approximate the uncertain terms in the AUVs trajectory tracking control system. Combining the bounded estimate, smoothing functions with parameter adaptive technique, the problem of unknown dead zone, actuator fault and input quantization are addressed. Finally, a practical fixed-time adaptive NN trajectory tracking control law is constructed under the backstepping design framework. The theoretical analysis and simulation results show the effectiveness of the proposed control scheme. This work can be extended to multiple-input-multiple-output nonlinear systems. In future studies, we will conduct experiments in the laboratory using a small AUV to validate the effectiveness of the trajectory tracking control scheme we have developed, and further event-triggered control could be considered.

DECLARATION OF COMPETING INTEREST

The authors declare that they have no known competing financial interests or personal relationships that could have appeared to influence the work reported in this article.

REFERENCES

[1] Y. Ma, Z. Nie, S. Hu, Z. Li, R. Malekian, and M. Sotelo, ''Fault detection filter and controller co-design for unmanned surface vehicles under DoS attacks,'' *IEEE Trans. Intell. Transp. Syst.*, vol. 22, no. 3, pp. 1422–1434, Mar. 2021.

[2] Y. Ma, M. Hu, and X. Yan, ''Multi-objective path planning for unmanned surface vehicle with currents effects,'' *ISA Trans.*, vol. 75, pp. 137–156, Apr. 2018.

[3] G. Zhu, Y. Ma, Z. Li, R. Malekian, and M. Sotelo, ''Dynamic event-triggered adaptive neural output feedback control for MSVs using composite learning,'' *IEEE Trans. Intell. Transp. Syst.*, vol. 24, no. 1, pp. 787–800, Jan. 2023.

[4] S. Liu, Y. Liu, X. Liang, and N. Wang, ''Uncertainty observation-based adaptive succinct fuzzy-neuro dynamic surface control for trajectory tracking of fully actuated underwater vehicle system with input saturation,'' *Nonlinear Dyn.*, vol. 98, no. 3, pp. 1683–1699, Oct. 2019.

[5] H. Ye, M. Chen, and Q. Zeng, ''Horizontal motion tracking control for an underwater vehicle with environmental disturbances,'' in *Proc. 36th Chin. Control Conf. (CCC)*, Dalian, China, Jul. 2017, pp. 4952–4957.

[6] X. Yang, J. Yan, C. Hua, and X. Guan, ''Trajectory tracking control of autonomous underwater vehicle with unknown parameters and external disturbances,'' *IEEE Trans. Syst., Man, Cybern., Syst.*, vol. 51, no. 2, pp. 1054–1063, Feb. 2021.

[7] R. Cui, X. Zhang, and D. Cui, ''Adaptive sliding-mode attitude control for autonomous underwater vehicles with input nonlinearities,'' *Ocean Eng.*, vol. 123, pp. 45–54, Sep. 2016.

[8] L. Qiao and W. Zhang, ''Adaptive second-order fast nonsingular terminal sliding mode tracking control for fully actuated autonomous underwater vehicles,'' *IEEE J. Ocean. Eng.*, vol. 44, no. 2, pp. 363–385, Apr. 2019.

[9] L. Qiao and W. Zhang, ''Trajectory tracking control of AUVs via adaptive fast nonsingular integral terminal sliding mode control,'' *IEEE Trans. Ind. Informat.*, vol. 16, no. 2, pp. 1248–1258, Feb. 2020.

[10] X. Wang, Y. Cao, B. Niu, and Y. Song, ''A novel bipartite consensus tracking control for multiagent systems under sensor deception attacks,'' *IEEE Trans. Cybern.*, vol. 53, no. 9, pp. 5984–5993, Sep. 2023.

[11] X. Wang, B. Niu, H. Wang, X. Zhao, and W. Chen, ''Prescribed performance-based finite-time consensus technology of nonlinear multiagent systems and application to FDPs,'' *IEEE Trans. Circuits Syst. II, Exp. Briefs*, vol. 70, no. 2, pp. 591–595, Feb. 2023.

[12] L. Cao, Y. Pan, H. Liang, and T. Huang, ''Observer-based dynamic event-triggered control for multiagent systems with time-varying delay,'' *IEEE Trans. Cybern.*, vol. 53, no. 5, pp. 3376–3387, May 2023.

[13] Y. Wang, B. Jiang, Z.-G. Wu, S. Xie, and Y. Peng, ''Adaptive sliding mode fault-tolerant fuzzy tracking control with application to unmanned marine vehicles,'' *IEEE Trans. Syst., Man, Cybern., Syst.*, vol. 51, no. 11, pp. 6691–6700, Nov. 2021.

[14] G. Zhu, Y. Ma, Z. Li, R. Malekian, and M. Sotelo, ''Adaptive neural output feedback control for MSVs with predefined performance,'' *IEEE Trans. Veh. Technol.*, vol. 70, no. 4, pp. 2994–3006, Apr. 2021.

[15] J. Li, J. Du, and C. L. P. Chen, ''Command-filtered robust adaptive NN control with the prescribed performance for the 3-D trajectory tracking of underactuated AUVs,'' *IEEE Trans. Neural Netw. Learn. Syst.*, vol. 33, no. 11, pp. 6545–6557, Nov. 2022.

[16] J. Li, J. Du, Y. Sun, and F. L. Lewis, ''Robust adaptive trajectory tracking control of underactuated autonomous underwater vehicles with prescribed performance,'' *Int. J. Robust Nonlinear Control*, vol. 29, no. 14, pp. 4629–4643, Sep. 2019.

[17] K. Shojaei and M. M. Arefi, ''On the neuro-adaptive feedback linearising control of underactuated autonomous underwater vehicles in three-dimensional space,'' *IET Control Theory Appl.*, vol. 9, no. 8, pp. 1264–1273, May 2015.

[18] O. Elhaki and K. Shojaei, ''Neural network-based target tracking control of underactuated autonomous underwater vehicles with a prescribed performance,'' *Ocean Eng.*, vol. 167, pp. 239–256, Nov. 2018.

[19] J. Liu and J. Du, ''Composite learning tracking control for underactuated autonomous underwater vehicle with unknown dynamics and disturbances in three-dimension space,'' *Appl. Ocean Res.*, vol. 112, Jul. 2021, Art. no. 102686.

[20] X. Huang, Y. Yan, and Z. Huang, ''Finite-time control of underactuated spacecraft hovering,'' *Control Eng. Pract.*, vol. 68, pp. 46–62, Nov. 2017.

[21] X. Jin, ''Adaptive finite-time fault-tolerant tracking control for a class of MIMO nonlinear systems with output constraints,'' *Int. J. Robust Nonlinear Control*, vol. 27, no. 5, pp. 722–741, Mar. 2017.

[22] Y. Liu, X. Liu, Y. Jing, H. Wang, and X. Li, ''Annular domain finite-time connective control for large-scale systems with expanding construction,'' *IEEE Trans. Syst., Man, Cybern., Syst.*, vol. 51, no. 10, pp. 6159–6169, Oct. 2021.

[23] Z. Gao and G. Guo, ''Fixed-time sliding mode formation control of AUVs based on a disturbance observer,'' *IEEE/CAA J. Autom. Sinica*, vol. 7, no. 2, pp. 539–545, Mar. 2020.

[24] H. Sun, G. Zong, J. Cui, and K. Shi, ''Fixed-time sliding mode output feedback tracking control for autonomous underwater vehicle with prescribed performance constraint,'' *Ocean Eng.*, vol. 247, Mar. 2022, Art. no. 110673.

[25] Y. Liu, D. Yao, L. Wang, and S. Lu, ''Distributed adaptive fixed-time robust platoon control for fully heterogeneous vehicles,'' *IEEE Trans. Syst., Man, Cybern., Syst.*, vol. 53, no. 1, pp. 264–274, Jan. 2023.

[26] G. Che and Z. Yu, ''Neural-network estimators based fault-tolerant tracking control for AUV via ADP with rudders faults and ocean current disturbance,'' *Neurocomputing*, vol. 411, pp. 442–454, Oct. 2020.

[27] C. Zhu, B. Huang, B. Zhou, Y. Su, and E. Zhang, ''Adaptive model-parameter-free fault-tolerant trajectory tracking control for autonomous underwater vehicles,'' *ISA Trans.*, vol. 114, pp. 57–71, Aug. 2021.

[28] H. Liang, L. Chen, Y. Pan, and H.-K. Lam, ''Fuzzy-based robust precision consensus tracking for uncertain networked systems with cooperative–antagonistic interactions,'' *IEEE Trans. Fuzzy Syst.*, vol. 31, no. 4, pp. 1362–1376, Apr. 2023.

[29] Z. Zuo, J. Song, W. Wang, and Z. Ding, ''Adaptive backstepping control of uncertain sandwich-like nonlinear systems with deadzone nonlinearity,'' *IEEE Trans. Syst., Man, Cybern., Syst.*, vol. 52, no. 11, pp. 7268–7278, Nov. 2022.

[30] C. Li, X. Yang, and B. Xiao, ''Adaptive attitude tracking control of a 3-degrees-of-freedom experimental helicopter with actuator dead-zone,'' *Proc. Inst. Mech. Eng. I, J. Syst. Control Eng.*, vol. 233, no. 1, pp. 91–99, Jan. 2019.

[31] L. Ding, S. Li, H. Gao, Y.-J. Liu, L. Huang, and Z. Deng, ''Adaptive neural network-based finite-time online optimal tracking control of the nonlinear system with dead zone,'' *IEEE Trans. Cybern.*, vol. 51, no. 1, pp. 382–392, Jan. 2021.

[32] W. He, B. Huang, Y. Dong, Z. Li, and C.-Y. Su, ''Adaptive neural network control for robotic manipulators with unknown deadzone,'' *IEEE Trans. Cybern.*, vol. 48, no. 9, pp. 2670–2682, Sep. 2018.

[33] M. L. Corradini and G. Orlando, ''Robust quantized feedback stabilization of linear systems,'' *Automatica*, vol. 44, no. 9, pp. 2458–2462, Sep. 2008.

[34] H. Sun, L. Hou, G. Zong, and X. Yu, ''Fixed-time attitude tracking control for spacecraft with input quantization,'' *IEEE Trans. Aerosp. Electron. Syst.*, vol. 55, no. 1, pp. 124–134, Feb. 2019.

[35] P. Li, Z. Song, Z. Wang, and W. Liu, "Fixed-time consensus for disturbed multiple Euler–Lagrange systems with connectivity preservation and quantized input," *Appl. Math. Comput.*, vol. 380, Sep. 2020, Art. no. 125303.

[36] H. Liang, Y. Zhang, T. Huang, and H. Ma, "Prescribed performance cooperative control for multiagent systems with input quantization," *IEEE Trans. Cybern.*, vol. 50, no. 5, pp. 1810–1819, May 2020.

[37] J. Hu, X. Sun, and L. He, "Formation tracking for nonlinear multi-agent systems with input and output quantization via adaptive output feedback control," *J. Syst. Sci. Complex.*, vol. 33, no. 2, pp. 401–425, Apr. 2020.

[38] F. Cheng, H. Wang, G. Zong, B. Niu, and X. Zhao, "Adaptive finite-time command-filtered control for switched nonlinear systems with input quantization and output constraints," *Circuits, Syst., Signal Process.*, vol. 42, no. 1, pp. 147–172, Jan. 2023.

[39] J. Zhou, C. Wen, W. Wang, and F. Yang, "Adaptive backstepping control of nonlinear uncertain systems with quantized states," *IEEE Trans. Autom. Control*, vol. 64, no. 11, pp. 4756–4763, Nov. 2019.

[40] B. Huang, B. Zhou, S. Zhang, and C. Zhu, "Adaptive prescribed performance tracking control for underactuated autonomous underwater vehicles with input quantization," *Ocean Eng.*, vol. 221, Feb. 2021, Art. no. 108549.

[41] Y. H. Choi and S. J. Yoo, "Distributed quantized feedback design strategy for adaptive consensus tracking of uncertain strict-feedback nonlinear multiagent systems with state quantizers," *IEEE Trans. Cybern.*, vol. 52, no. 7, pp. 7069–7083, Jul. 2022.

[42] J. Li, J. Du, G. Zhu, and F. L. Lewis, "Simple adaptive trajectory tracking control of underactuated autonomous underwater vehicles under LOS range and angle constraints," *IET Control Theory Appl.*, vol. 14, no. 2, pp. 283–290, Jan. 2020.

[43] K. Shojaei, "Three-dimensional neural network tracking control of a moving target by underactuated autonomous underwater vehicles," *Neural Comput. Appl.*, vol. 31, no. 2, pp. 509–521, Feb. 2019.

[44] X. Qi and Z.-J. Cai, "Three-dimensional formation control based on filter backstepping method for multiple underactuated underwater vehicles," *Robotica*, vol. 35, no. 8, pp. 1690–1711, Aug. 2017.

[45] X. Qi and Z.-J. Cai, "Three-dimensional formation control based on nonlinear small gain method for multiple underactuated underwater vehicles," *Ocean Eng.*, vol. 151, pp. 105–114, Mar. 2018.

[46] Z. Zheng, M. Feroskhan, and L. Sun, "Adaptive fixed-time trajectory tracking control of a stratospheric airship," *ISA Trans.*, vol. 76, pp. 134–144, May 2018.

[47] C. Wang and Y. Lin, "Decentralized adaptive tracking control for a class of interconnected nonlinear time-varying systems," *Automatica*, vol. 54, pp. 16–24, Apr. 2015.

[48] M. M. Polycarpou, "Stable adaptive neural control scheme for nonlinear systems," *IEEE Trans. Autom. Control*, vol. 41, no. 3, pp. 447–451, Mar. 1996.

[49] J. Na, S. Wang, Y.-J. Liu, Y. Huang, and X. Ren, "Finite-time convergence adaptive neural network control for nonlinear servo systems," *IEEE Trans. Cybern.*, vol. 50, no. 6, pp. 2568–2579, Jun. 2020.

[50] S. S. Ge and J. Wang, "Robust adaptive neural control for a class of perturbed strict feedback nonlinear systems," *IEEE Trans. Neural Netw.*, vol. 13, no. 6, pp. 1409–1419, Nov. 2002.

[51] J. Zhou, C. Wen, and W. Wang, "Adaptive control of uncertain nonlinear systems with quantized input signal," *Automatica*, vol. 95, pp. 152–162, Sep. 2018.

[52] C. Zhu, H. Sun, and L. Hou, "Anti-disturbance attitude quantized control of flexible spacecraft via a triggering and quantization joint dynamic event-triggered mechanism," *Aerosp. Sci. Technol.*, vol. 136, May 2023, Art. no. 108191.

[53] N. Elia and S. K. Mitter, "Stabilization of linear systems with limited information," *IEEE Trans. Autom. Control*, vol. 46, no. 9, pp. 1384–1400, Sep. 2001.

[54] Z. Zhao, J. Zhang, Z. Liu, W. He, and K.-S. Hong, "Adaptive quantized fault-tolerant control of a 2-DOF helicopter system with actuator fault and unknown dead zone," *Automatica*, vol. 148, Feb. 2023, Art. no. 110792.

[55] Z. Liu, F. Wang, Y. Zhang, and C. L. P. Chen, "Fuzzy adaptive quantized control for a class of stochastic nonlinear uncertain systems," *IEEE Trans. Cybern.*, vol. 46, no. 2, pp. 524–534, Feb. 2016.

[56] K. Zhao and J. Chen, "Adaptive neural quantized control of MIMO nonlinear systems under actuation faults and time-varying output constraints," *IEEE Trans. Neural Netw. Learn. Syst.*, vol. 31, no. 9, pp. 3471–3481, Sep. 2020.

HUARAN YAN received the B.E. degree in navigational technology from the Wuhan University of Technology, Wuhan, China, in 2009, and the M.E. degree in traffic information engineering and control from Dalian Maritime University, Dalian, in 2011. He is currently pursuing the Ph.D. degree in vehicle operation engineering with the Merchant Marine College, Shanghai Maritime University.

He is a Lecturer with the Merchant Marine College, Shanghai Maritime University. His current research interests include navigation safety, intelligent control, and adaptive control with simulation of ship dynamics.

YINGJIE XIAO received the M.E. degree in navigational technology from Shanghai Shipping University, China, in 1982.

In recent years, he has presided over and participated in dozens of national, provincial, and ministerial level vertical, and more than 640 marine engineering navigation demonstrations, control simulation, engineering plan optimization, emergency plans, and other projects, with a total research fund of more than 100 million yuan. His current research interests include ship traffic and safety and navigation technology. He has won the Third Prize in the China Navigation Science and Technology Award, the Shanghai Yucai Award, the Third Prize in the China Port Science and Technology Progress Award, the Second Prize in the China Navigation Science and Technology Award, and the Excellent Teacher Award of Baosteel Education Fund.

HONGGANG ZHANG received the B.E. and M.E. degrees in navigational technology from the Wuhan University of Technology, Wuhan, China, in 2009 and 2011, respectively.

He is currently a Lecturer with the Marine College, Zhejiiang Ocean University. His current research interests include navigation safety and intelligent control with simulation of ship dynamics.